NACA RM A57A25

NACA

RESEARCH MEMORANDUM

LATERAL-DIRECTIONAL AERODYNAMIC CHARACTERISTICS OF SEVERAL COPLANAR TRIPLE-BODY MISSILE CONFIGURATIONS AT MACH NUMBERS FROM 0.6 TO 1.4

By Stuart L. Treon and Earl D. Knechtel

Ames Aeronautical Laboratory
Moffett Field, Calif.

NATIONAL ADVISORY COMMITTEE
FOR AERONAUTICS
WASHINGTON

April 10, 1957
Declassified October 28, 1960

NATIONAL ADVISORY COMMITTEE FOR AERONAUTICS

RESEARCH MEMORANDUM

LATERAL-DIRECTIONAL AERODYNAMIC CHARACTERISTICS OF SEVERAL COPLANAR TRIPLE-BODY MISSILE CONFIGURATIONS AT MACH NUMBERS FROM 0.6 to 1.4

By Stuart L. Treon and Earl D. Knechtel

SUMMARY

An experimental investigation was conducted to determine the lateral-directional aerodynamic characteristics at transonic speeds of missile configurations having three blunted cone-cylinder bodies. Modifications of the basic model were tested to determine the effects of relative lengths of the bodies as well as the effects of seals between the cylindrical parts of the bodies. Cross-wind force, drag, yawing moment, and rolling moment were measured through a sideslip-angle range from -8° to $+8^{\circ}$ at selected angles of attack up to 8° for ten Mach numbers from 0.6 to 1.4 and at a constant Reynolds number of 5.5×10^{6} based on average body length.

The results of the investigation indicate that all models tested had lateral centers of pressure located far ahead of the centroid of plan-form area and farther forward than the corresponding centers of lift previously determined (NACA RM A56H31) for these configurations. The lateral centers of pressure tended to move forward with an increase in Mach number from 0.6 to 1.2, then rearward with further increase in Mach number. Cross-wind-force parameter tended to become more negative with increasing Mach number, this effect becoming more pronounced with increased angle of sideslip and angle of attack. All models were found to have a positive dihedral effect, which increased with angle of attack but was relatively less affected by changes in Mach number or angle of sideslip.

For triple-body configurations having the same average body length, the effects of changes in the relative lengths of the bodies were generally insignificant with respect to the lateral-directional characteristics. Sealing the gap between bodies generally tended to cause a slight rearward shift in the lateral center of pressure and an increase in positive dihedral effect.

Comparison of experimental results with available theory indicates that, when flow interference is neglected, slender-body theory or a combination of slender-body and viscous crossflow theory greatly overestimates the magnitudes of both cross-wind force and yawing moment.

INTRODUCTION

Research interest in the long-range ballistic-type missile has been concentrated in the past on fin-stabilized, tandem-mounted, multistage rocket configurations. Further consideration of this research problem, however, has indicated a possible alternate solution consisting of the lateral-staging arrangement of parallel bodies as discussed in references 1 and 2.

This report is concerned with the lateral-directional characteristics at transonic speeds of some of the triple-body configurations for which the longitudinal characteristics were presented in reference 1.

NOTATION

C_C cross-wind force coefficient, $\frac{\text{cross-wind force}}{qS}$

C_D drag coefficient, $\frac{\text{drag}}{qS}$

C_l rolling-moment coefficient about axis of center body, $\frac{\text{rolling moment}}{qSd}$

C_n yawing-moment coefficient about point 6.32 inches ahead of base of center body, $\frac{\text{yawing moment}}{qSd}$

d body diameter

M free-stream Mach number

q free-stream dynamic pressure

S total base area of model, exclusive of seals

α angle of attack, deg

β angle of sideslip, deg

Model Designations

1	coplanar bodies of equal length
2	coplanar bodies, center body short
3	coplanar bodies, center body long
S	seals between cylindrical bodies

APPARATUS AND MODELS

This investigation was conducted in the Ames 2- by 2-foot transonic wind tunnel described in reference 3. The ventilated test section of this facility allows continuous, choke-free operation to Mach number 1.4.

The dimensions of the six configurations of this investigation are shown in figure 1. Each had three parallel, coplanar bodies comprised of cone-cylinders 1.50 inches in diameter, connected by modified-wedge struts across the 0.10-inch gap between the cylindrical portions of the bodies. The identical nose cones were derived from a basic cone having a length-to-diameter ratio of 4, which was blunted by truncating 20 percent of the nose length and rounding off to a hemispherical nose, in accordance with the results of recent investigations of drag and aerodynamic heating of cone-cylinders (refs. 4 and 5). Models 1, 2, and 3 differed in nose arrangement, or relative lengths of the three bodies, while average body length, total volume, and surface area were held constant. A corresponding set, models 1S, 2S, and 3S, had seals between the cylindrical bodies. The models were mounted in the test section on a sting-supported internal strain-gage balance as shown in figure 2.

TESTS AND DATA REDUCTION

Cross-wind force, drag, yawing moment, and rolling moment were measured through a sideslip range from -8° to $+8^{\circ}$ and at ten Mach numbers from 0.6 to 1.4 at constant angles of attack. The angles of attack of the investigation were 0° for configurations 1, 2, 3, and 1S, 4° for all six configurations, and 8° for configurations 1 and 1S. A Reynolds number of 5.5×10^{6}, based on average body length, was maintained throughout the tests.

The force coefficients were referred to the wind axes and were based on the total model base area. The moment coefficients were referred to the stability axes and were based on the total model base area and the

base diameter of one body. The moment reference point was located at the centroid of plan-form area of configuration 1 (6.32 inches ahead of base) in the horizontal plane of symmetry. Angles of attack were referred to the common plane of the body axes and angles of sideslip were referred to the model vertical plane of symmetry.

Corrections were applied to (1) the angles of attack and sideslip to account for deflections of the sting and balance resulting from static aerodynamic loads, (2) the drag to adjust for the difference between the measured model base pressures and free-stream static pressure, and (3) the yawing moment to account for differences between the base pressures of the leading and trailing bodies.

Subsonic wall-interference corrections calculated according to the method of reference 6 were found to be small enough to neglect for the present case, in which the ratio of model-to-tunnel cross-sectional area was approximately 0.009. No corrections were made for the effects of reflected shock waves at low supersonic speeds. Corrections for drag buoyancy and air-stream angularity were unnecessary, since they were known to be less than the probable errors in measuring drag and angle of attack, respectively.

Apart from the possible systematic errors caused by neglecting the aforementioned corrections, the data are considered to be repeatable within the following random errors of measurement as determined by a root-mean-square analysis of the data scatter:

M	± 0.003
α	$\pm 0.03^{\circ}$
β	$\pm 0.03^{\circ}$
C_C	± 0.040
C_D	± 0.008
C_l	± 0.012
C_n	± 0.13

RESULTS AND DISCUSSION

Representative basic data plots are shown only for the three unsealed configurations at three of the ten test Mach numbers, since the results of the present investigation indicated that the shapes of the basic force and moment curves were not greatly influenced by changes in

Mach number or by addition of seals between the cylindrical bodies. These typical results (fig. 3) indicate the variations of cross-wind force, foredrag, yawing moment, and rolling moment with sideslip angle at Mach numbers of 0.60, 0.98, and 1.40 and at angles of attack of 0°, 4°, and 8°. A better comparison of the effects of configuration geometry and of Mach number is provided by the small but definite changes in the slopes of the basic force and moment curves. For this purpose, there are presented in figures 4, 5, and 6, respectively, the variations with Mach number of lateral center-of-pressure position, cross-wind-force parameter C_C/β, and rolling-moment-curve slope for all six configurations at constant angles of attack and sideslip. In the limiting case of $\beta = 0^{\circ}$ shown in figures 4(a) and 5(a), the values of cross-wind-force parameter and lateral center of pressure were evaluated by taking the slopes of the cross-wind-force and yawing-moment curves at $\beta = 0^{\circ}$.

Particularly noticeable was the forward position of the lateral center of pressure (fig. 4), indicative of static directional instability for all the model configurations at all sideslip angles, angles of attack, and Mach numbers of the investigation. These lateral centers of pressure were significantly farther forward than were the corresponding centers of lift shown in reference 1. A probable explanation of this stems from the different potential-flow interference effects in the two cases, as shown in the later section entitled "Comparison with Available Theory." Common to all the configurations was the general tendency of the lateral center of pressure to move forward as Mach number was increased from 0.6 to 1.2, followed by a rearward movement as Mach number was further increased to the test limit of 1.4. For all the configurations, the variations of cross-wind-force parameter C_C/β with the flow variables (fig. 5) were similar. The general trend of this parameter was to become more negative with increasing Mach number, this effect becoming slightly more pronounced with increase in sideslip angle and angle of attack. Positive dihedral effect (negative C_{l_β}), indicative of static stability in roll, was evident throughout the range of flow variables for all the configurations, as shown in figure 6. Although the dihedral effect was very small at $\alpha = 0^{\circ}$, it increased markedly with angle of attack. In comparison, the changes in C_{l_β} with Mach number and angle of sideslip were relatively slight.

Prominent features of the results shown in figures 4 to 6 are the deviations of most of the curves at Mach numbers from about 1.0 to 1.1. These deviations are attributed entirely to the reflection of pressure waves back onto the model from the tunnel walls. Similar, but considerably smaller deviations were noted in the longitudinal data of reference 1. The most probable explanation for the fact that the deviations in the lateral data are larger is that, in the case of the lateral-directional measurements, the outboard bodies were closer to the reflecting walls than in the case of the longitudinal measurements.

Effects of Relative Body Length

Relative body length, or the axial disposition of model volume, had no significant effect on the over-all lateral-directional characteristics as indicated by an examination of figures 4 through 6. For the more slender configuration 3, however, there was less variation of both center-of-pressure travel and cross-wind-force parameter between Mach numbers 1.0 and 1.1 (the range in which it was possible for wall-reflected shock waves to impinge on the models) than was apparant for configurations 1 and 2.

A noticeably lower drag rise from subsonic to supersonic Mach numbers was also evident for configuration 3 as indicated in the basic data (fig. 3) and discussed in detail in reference 1. The incremental difference in drag between models remained essentially constant with variation of sideslip angle.

Effects of Seals Between Bodies

The effect of sealing the gaps between the cylindrical portions of the bodies was generally not large and was not completely consistent, but certain trends were discernible. Addition of seals generally tended to cause a slight rearward shift of the lateral center of pressure (fig. 4), as contrasted with the slight forward shift in the center of lift shown in reference 1. In the present case, addition of seals also generally tended to cause an increased positive dihedral effect as indicated in figure 6. The cross-wind-force parameter (fig. 5) had generally similar values and characteristics for corresponding sealed and unsealed configurations, except for configurations 1 and 1S at small sideslip angles and moderate angles of attack.

Comparison With Available Theory

As in the case of the longitudinal characteristics of these configurations (ref. 1), it is of some interest to know how the experimental results compare with results calculated by available theoretical methods. In the absence of any known solution for the potential flow about yawed multiple-body configurations of the present type, the values of cross-wind force and yawing moment were calculated neglecting interference. The method employed the slender-body theory of references 7 and 8 for the potential loads on the nose cones and the viscous crossflow theory of reference 9 for the loads on the cylindrical bodies, in a manner analogous to the calculations of lift and pitching moment in reference 1. The assumption was made that viscous cross forces act only on the cylindrical

portions of the models, and these loads were calculated using the drag coefficients of two-dimensional cylinders of oval section (ref. 10) as an approximation to the crossflow drag coefficient of the triple-body model. The two-dimensional drag coefficients (0.3 for the triple body and 1.2 for the single body) were corrected for finite cylinder length as in reference 9.

In figure 7, typical cross-wind-force and yawing-moment results for configuration 1 are compared with values calculated using a combination of slender-body and viscous crossflow theory as well as slender-body theory alone. These comparisons indicate that calculation by either of these methods seriously overestimates the magnitude of both the cross-wind force and yawing moment of triple-body configurations. In the present case, as in reference 1, it is of help in examining these differences to show a similar comparison of experimental and calculated results for a single body of configuration 1. Such a comparison in figure 7 indicates generally good agreement of calculated cross-wind force and yawing moment with the experimental single-body results. For the triple-body configuration, however, the lack of agreement between the experimental and calculated curves can be attributed mainly to their differences in initial slope. The initial slopes of the calculated curves are obtained from the slender-body potential theory and, in coefficient form, are identical for single or multiple bodies when interference is neglected. Taken together, these facts indicate that potential-flow interference between adjacent cones probably caused the lack of agreement between experimental and calculated results for the triple-body configuration.

Investigation of the longitudinal characteristics of these triple-body models (ref. 1) indicated that potential-flow interference greatly increased the magnitudes of both the lift and pitching moment from those of three independent bodies. In contrast, the results of the present investigation show that the effect of interference on the lateral-directional characteristics was to reduce the magnitudes of both the cross-wind force and yawing moment. Consideration of the flow about closely spaced parallel cones yawed in the common plane of their axes indicates that such an effect of interference should be expected. The forward parts of the three cones are widely spaced relative to the local cone diameters, so potential loads on these portions should be relatively unaffected by interference between cones. However, over the rearward portions of the cones, where the greater part of the potential loading occurs, the cone diameters become increasingly large relative to their spacing. This can lead to reduction in the magnitude of the cross-wind force on the rearward part of the cones, since adjacent surfaces on yawed parallel cones tend to have pressure coefficients of opposite sign. In the present case, the resulting forward shift in center of lateral pressure was more than compensated by the large decrease in cross-wind force, resulting (fig. 7) in yawing moments much smaller in magnitude than those calculated neglecting interference.

CONCLUSIONS

The results of an experimental investigation of the lateral-directional aerodynamic characteristics of several coplanar triple-body missile configurations lead to the following conclusions:

1. All model configurations tested had lateral centers of pressure located far ahead of the centroid of plan-form area and significantly farther forward than the corresponding centers of lift previously determined. The lateral centers of pressure generally tended to move forward with an increase in Mach number from 0.6 to 1.2, then rearward with further increase in Mach number.

2. Cross-wind-force parameter C_C/β tended to become more negative with increasing Mach number, an effect which became more pronounced with increased angles of sideslip and attack.

3. Throughout the range of flow variables, all models were found to be statically stable in roll. This positive dihedral effect increased markedly with angle of attack, but was relatively less sensitive to changes in Mach number and angle of sideslip.

4. For triple-body configurations having the same average body length, changes in the lengths of individual bodies had no significant effect on the lateral-directional characteristics.

5. Addition of seals between the bodies tended to cause a slight rearward shift in the lateral center of pressure and an increase in positive dihedral effect.

6. Comparison of experimental results with available theory indicates that, when flow interference is neglected, either slender-body theory alone or a combination of slender-body and viscous crossflow theory greatly overestimates the magnitudes of both cross-wind force and yawing moment.

Ames Aeronautical Laboratory
National Advisory Committee for Aeronautics
Moffett Field, Calif., Jan. 25, 1957

REFERENCES

1. Knechtel, Earl D., and Andrea, Arvid N.: Aerodynamic Characteristics in Pitch of Several Triple-Body Missile Configurations at Mach Numbers From 0.6 to 1.4. NACA RM A56H31, 1956.

2. Cole, Dandridge M., and Epstein, L. Ivan: Interpretation of the Malina-Summerfield Criterion for Optimization of Multistage Rockets. Jour. American Rocket Society, vol. 26, no. 3, Mar. 1956, p. 188.

3. Spiegel, Joseph M., and Lawrence, Leslie F.: A Description of the Ames 2- by 2-Foot Transonic Wind Tunnel and Preliminary Evaluation of Wall Interference. NACA RM A55I21, 1956.

4. Sommer, Simon C., and Stark, James A.: The Effect of Bluntness on the Drag of Spherical-Tipped Truncated Cones of Fineness Ratio 3 at Mach Numbers 1.2 to 7.4. NACA RM A52B13, 1952.

5. Allen, H. Julian, and Eggers, A. J., Jr.: A Study of the Motion and Aerodynamic Heating of Missiles Entering the Earth's Atmosphere at High Supersonic Speeds. NACA RM A53D28, 1953.

6. Baldwin, Barrett S., Jr., Turner, John B., and Knechtel, Earl D.: Wall Interference in Wind Tunnels with Slotted and Porous Boundaries at Subsonic Speeds. NACA TN 3176, 1954 (Formerly NACA RM A53E29).

7. Munk, Max M.: The Aerodynamic Forces on Airship Hulls. NACA Rep. 184, 1924.

8. Tsien, Hsue-Shen: Supersonic Flow Over an Inclined Body of Revolution. Jour. Aero. Sci., vol. 5, no. 12, Oct. 1938, pp. 480-483.

9. Allen, H. Julian, and Perkins, Edward W.: Characteristics of Flow Over Inclined Bodies of Revolution. NACA RM A50L07, 1951.

10. Delany, Noel K., and Sorensen, Norman E.: Low-Speed Drag of Cylinders of Various Shapes. NACA TN 3038, 1953.

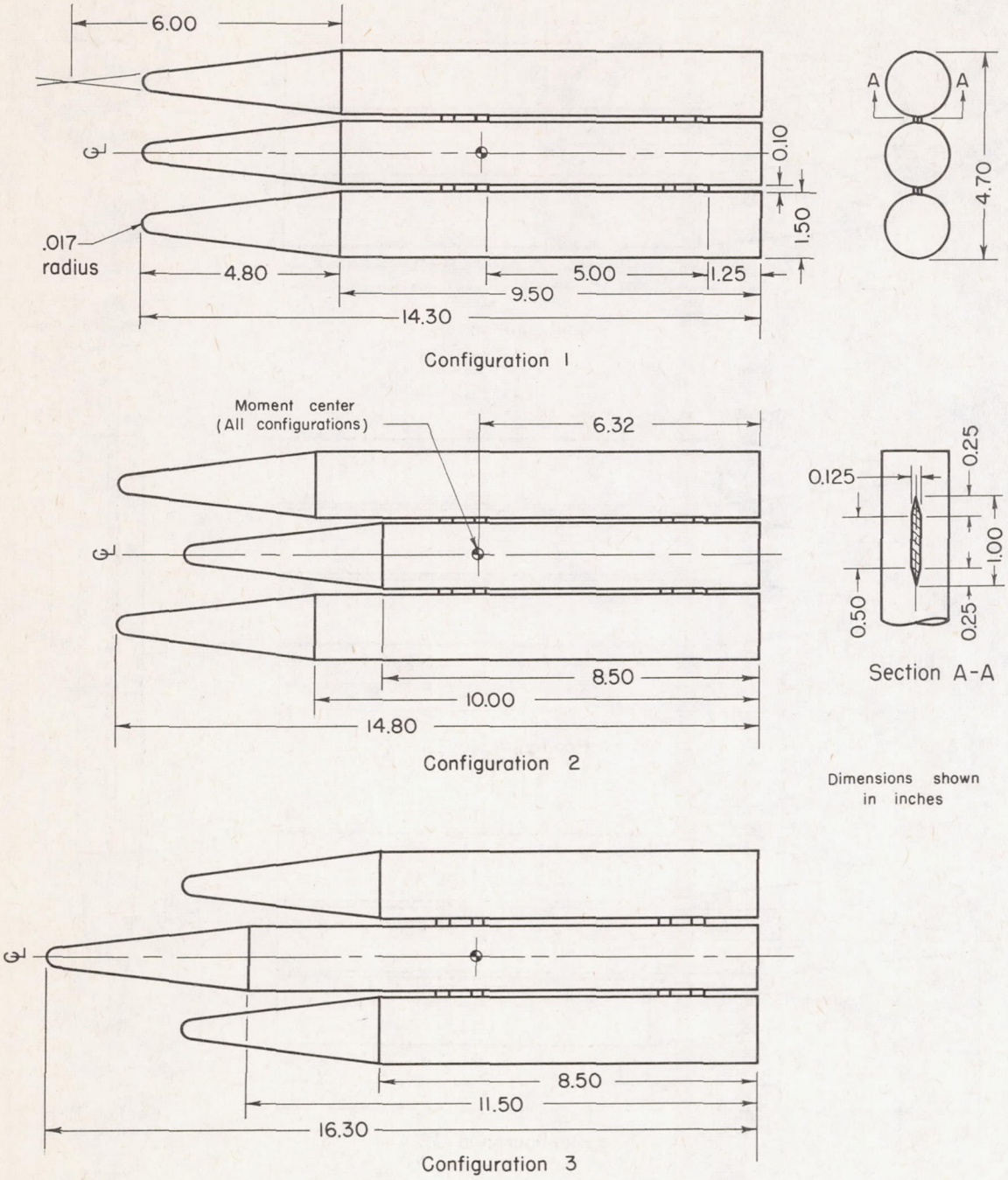

(a) Configurations 1, 2, and 3.

Figure 1.- Plan forms and geometric details of models.

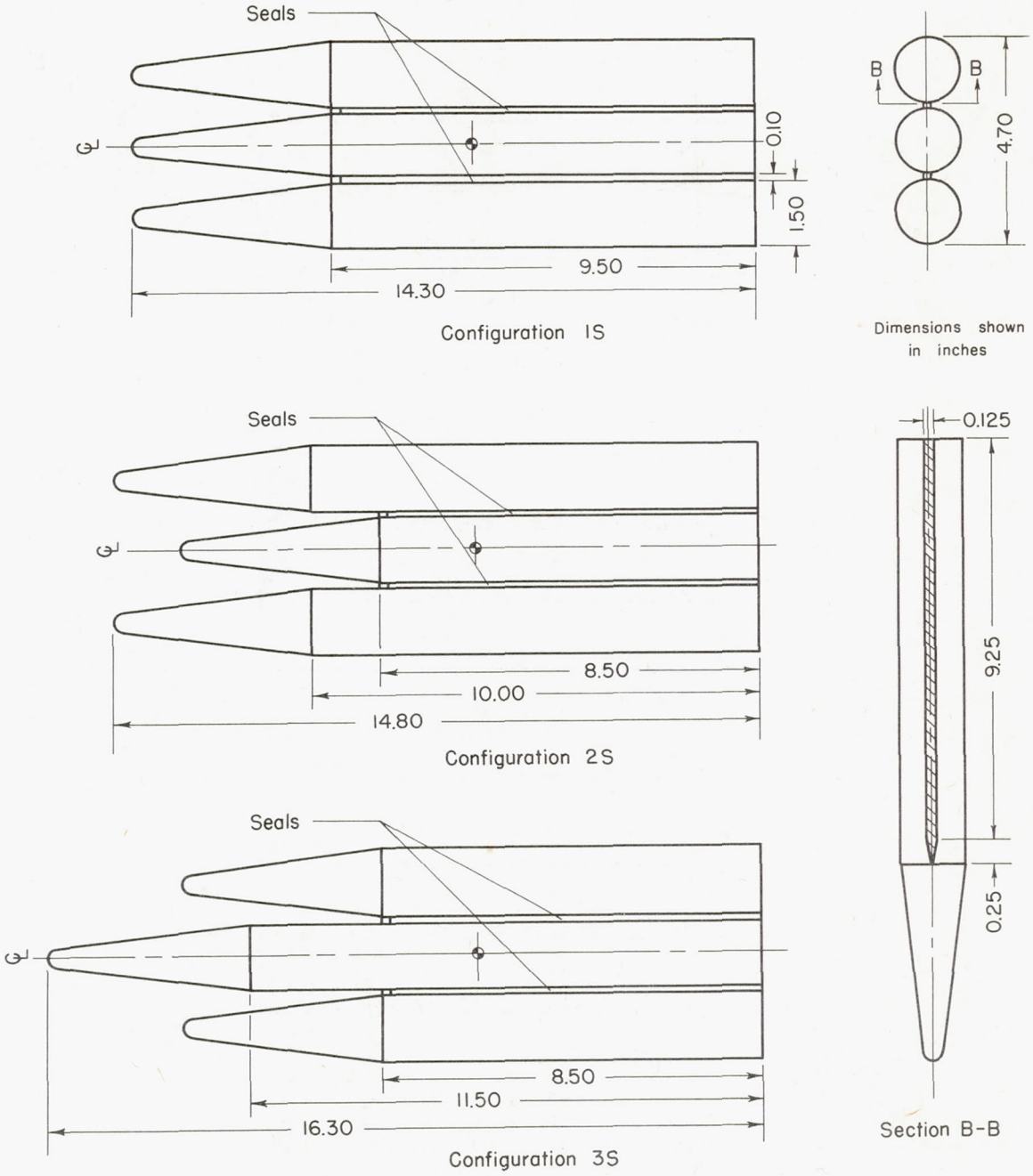

(b) Configurations 1S, 2S, and 3S.

Figure 1.- Concluded.

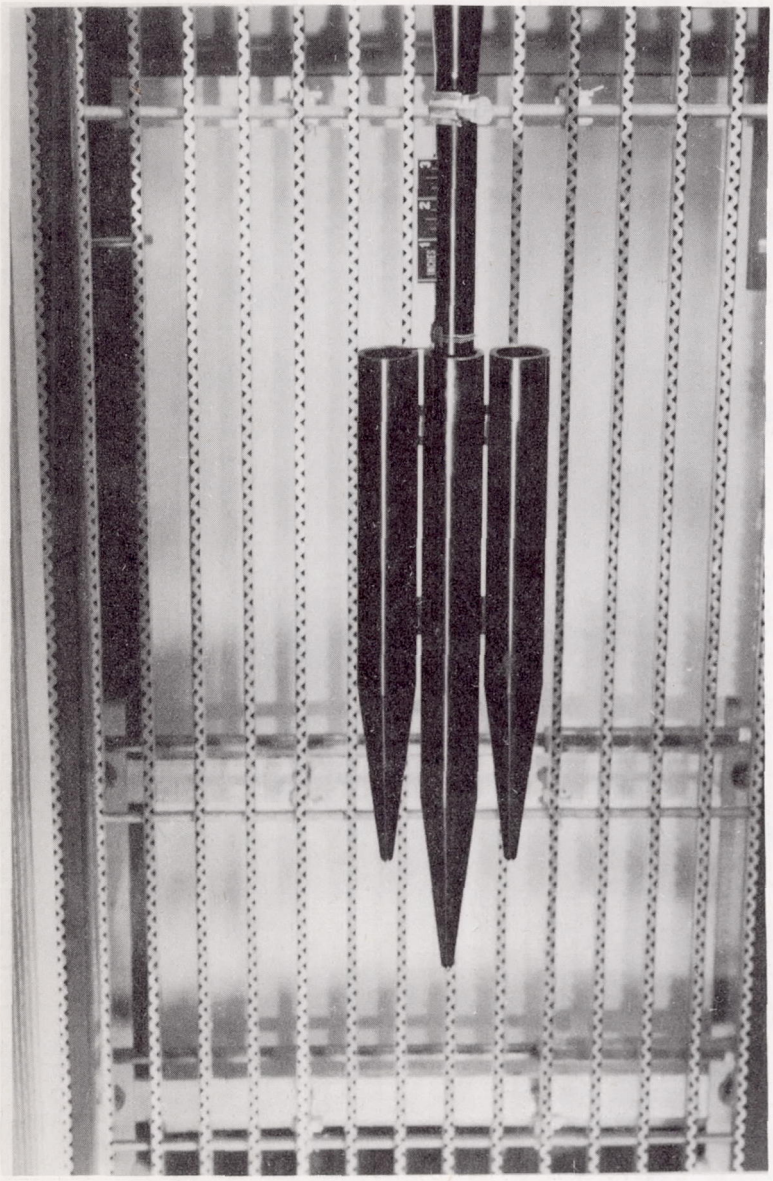

A-20684

Figure 2.- Typical model installed in the Ames 2-by 2-foot transonic wind tunnel.

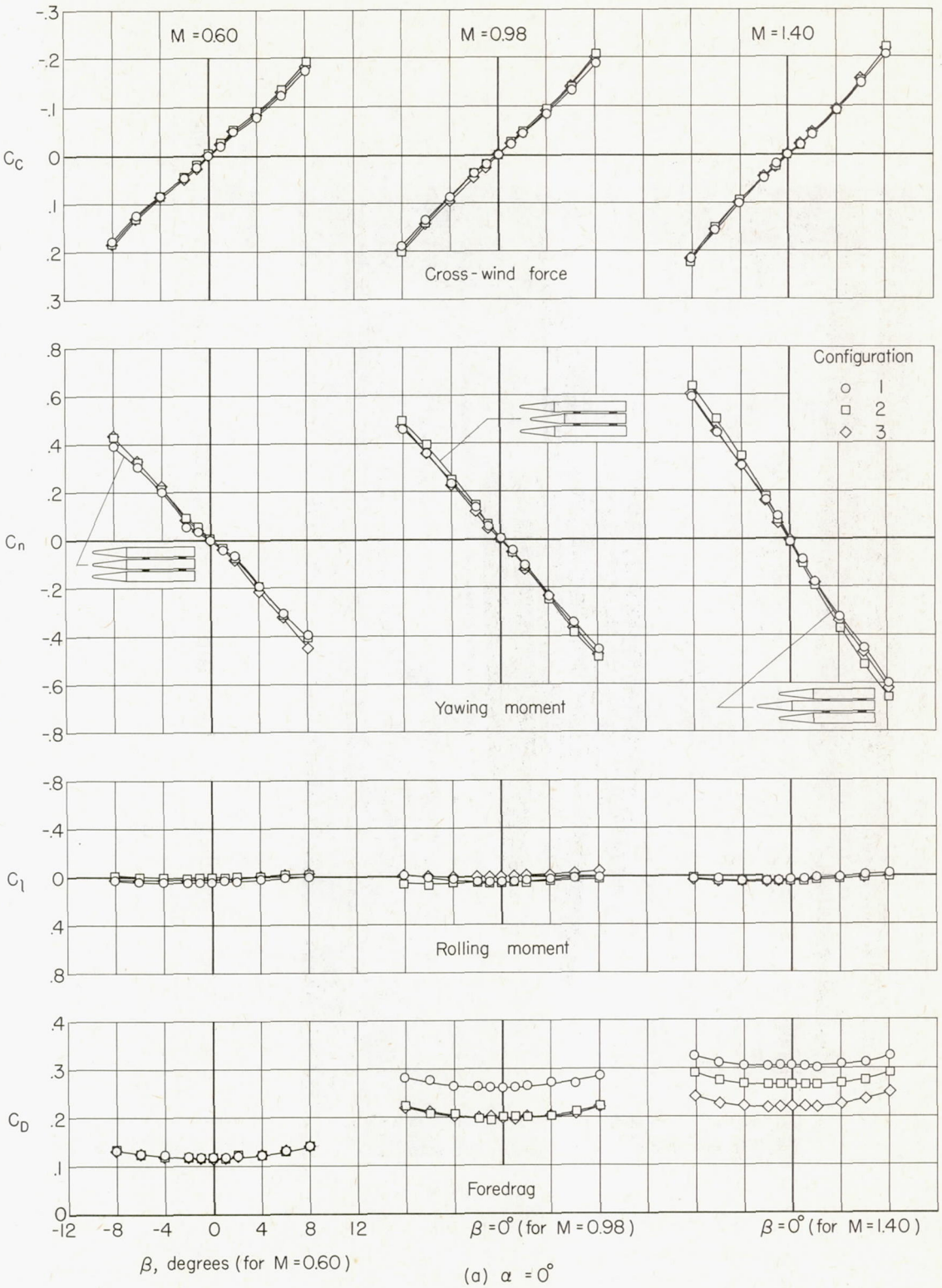

(a) $\alpha = 0°$

Figure 3.- Representative lateral-directional characteristics of triple-body missile configurations.

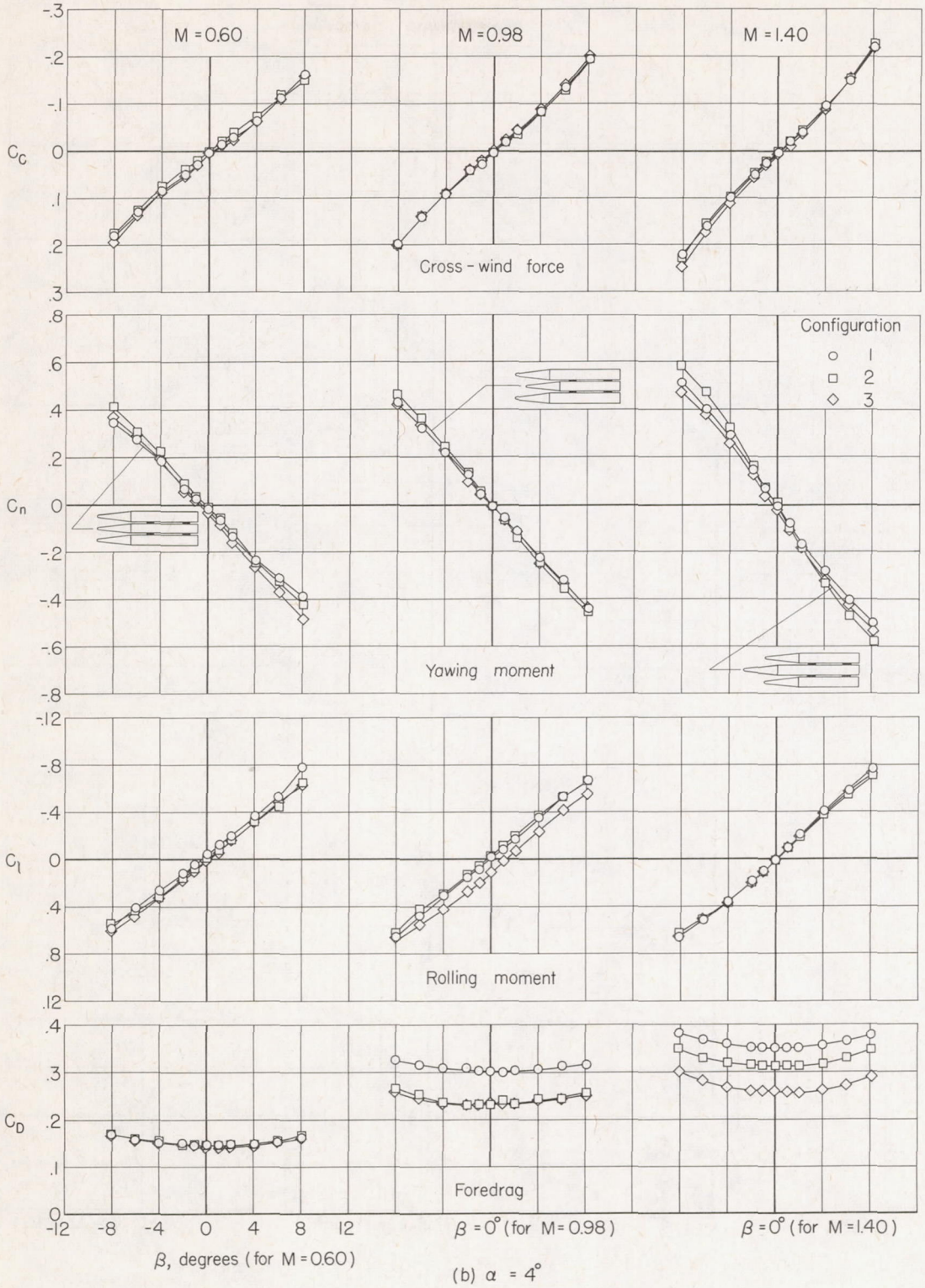

(b) $\alpha = 4°$

Figure 3.- Continued.

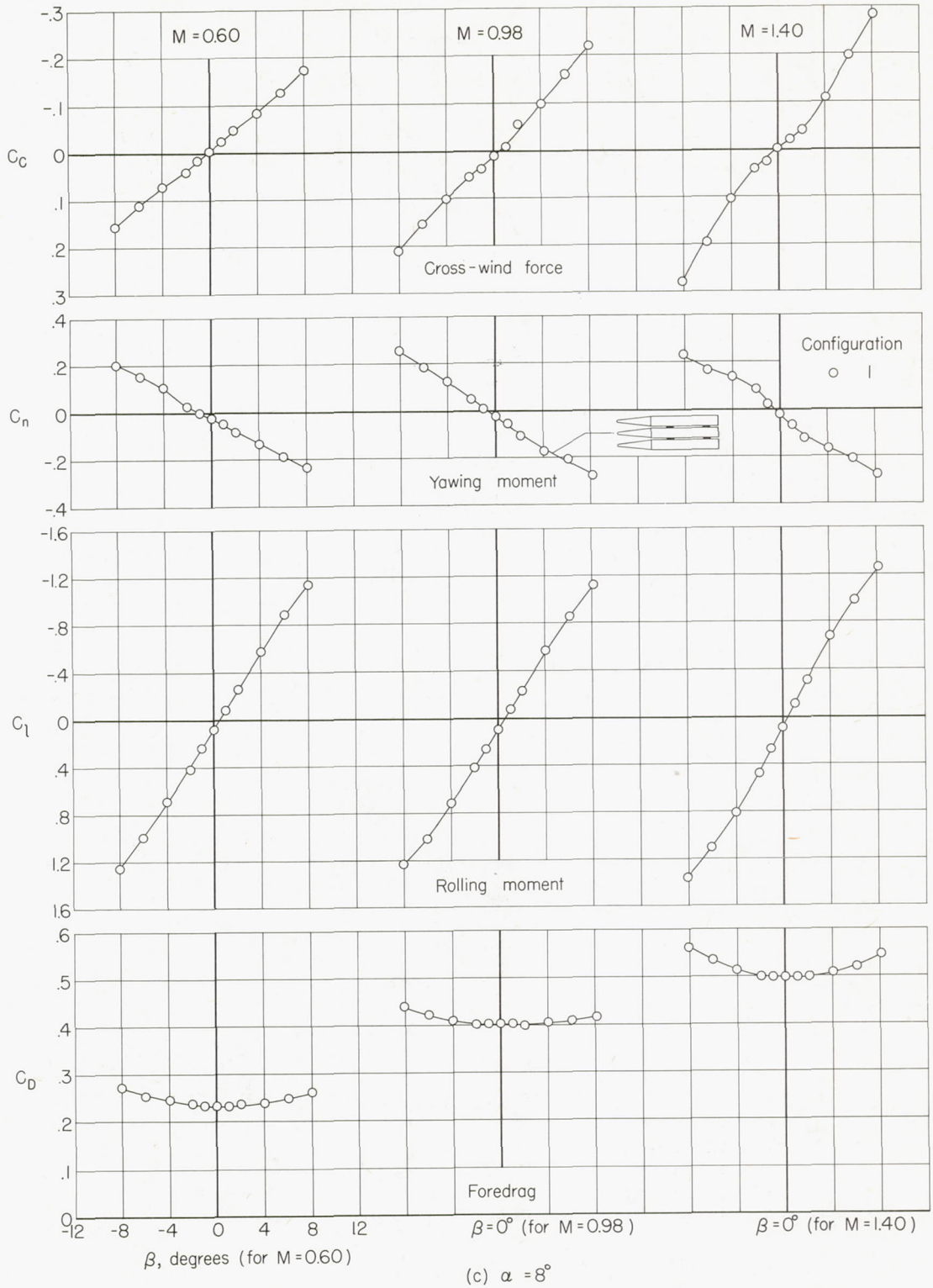

(c) $\alpha = 8°$

Figure 3. - Concluded.

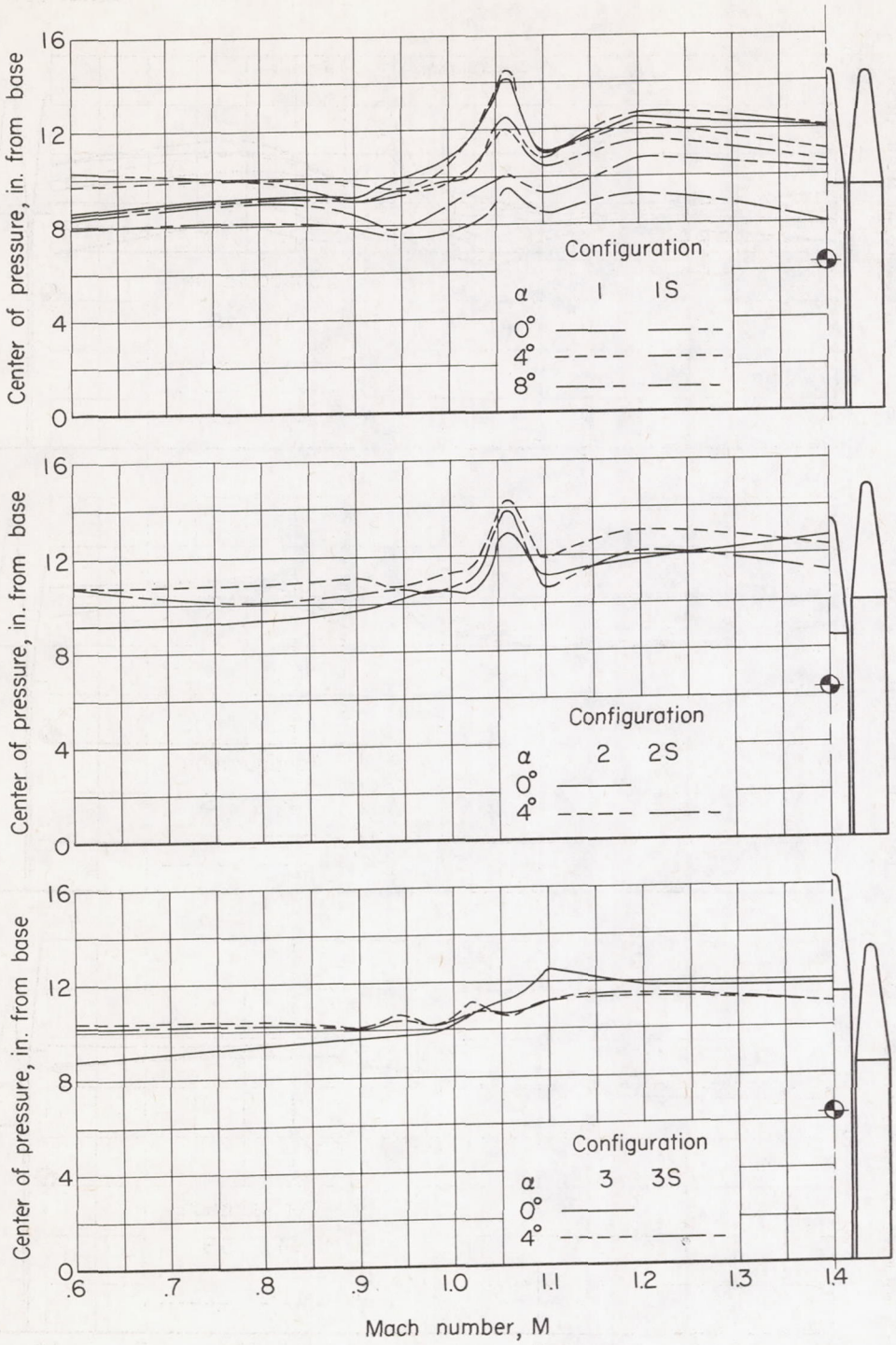

(a) $\beta = 0°$

Figure 4.- Variation of lateral center of pressure with Mach number at constant angles of attack and sideslip for several triple-body configurations.

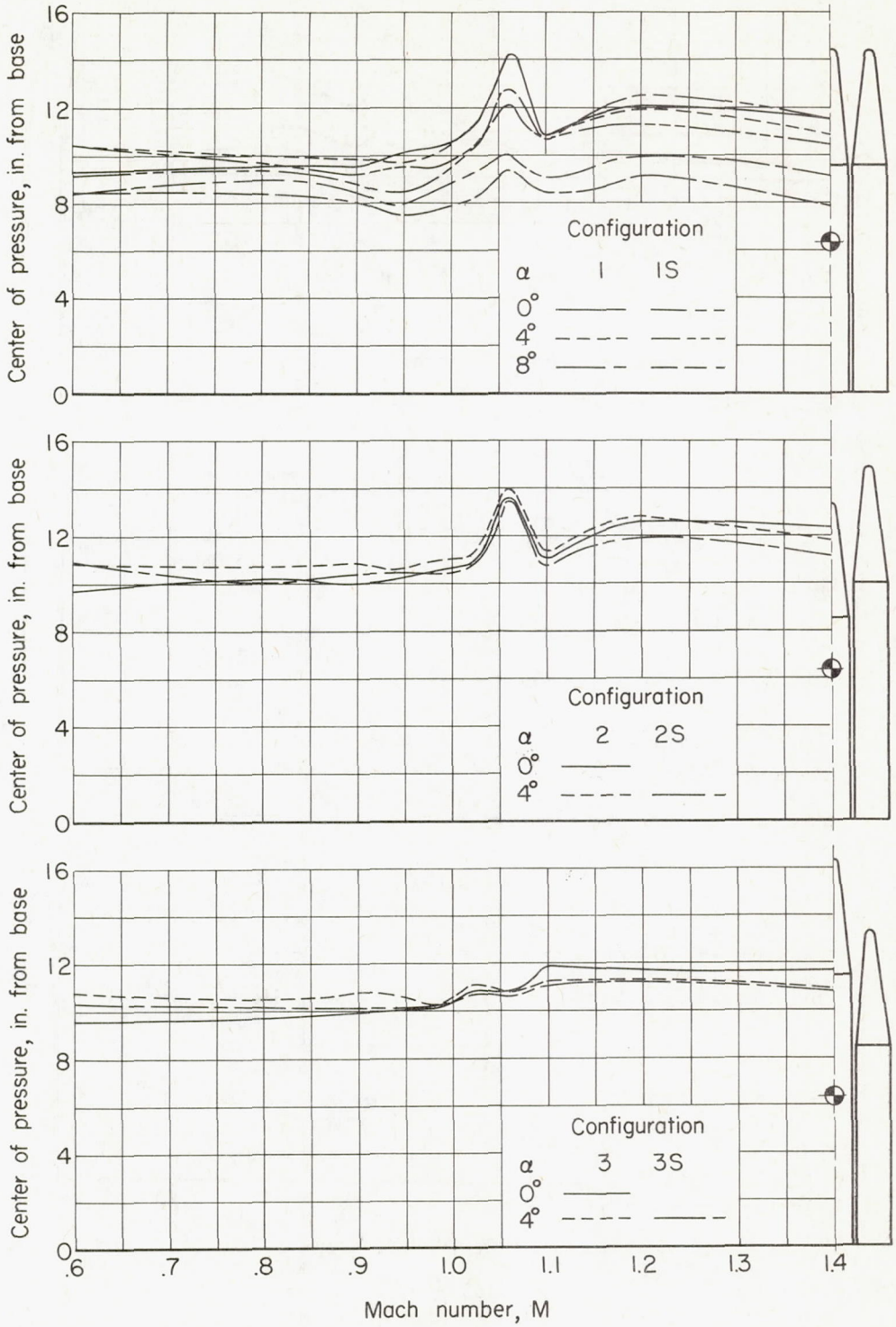

(b) $\beta = 3°$

Figure 4.- Continued.

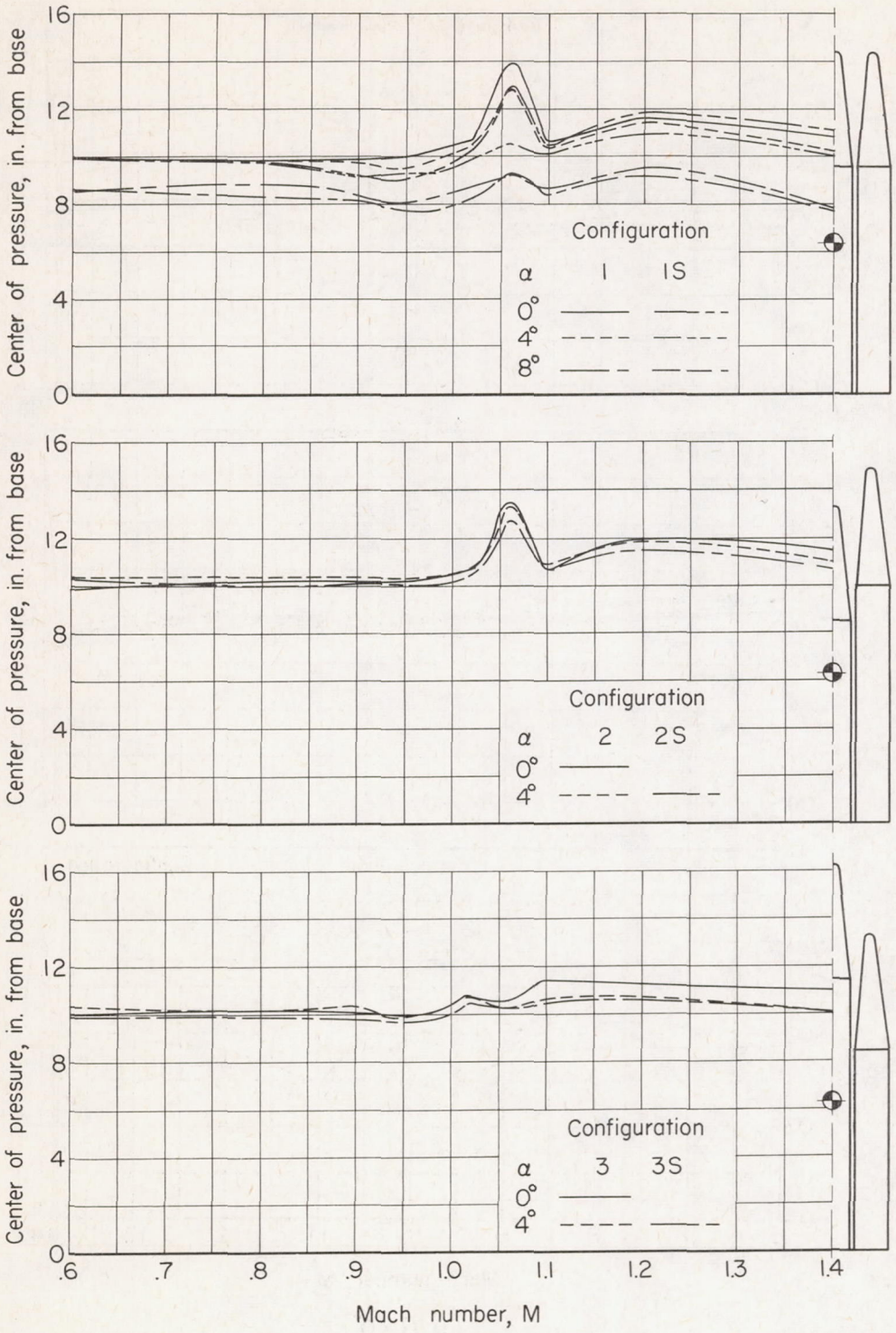

(c) $\beta = 6°$

Figure 4.- Concluded.

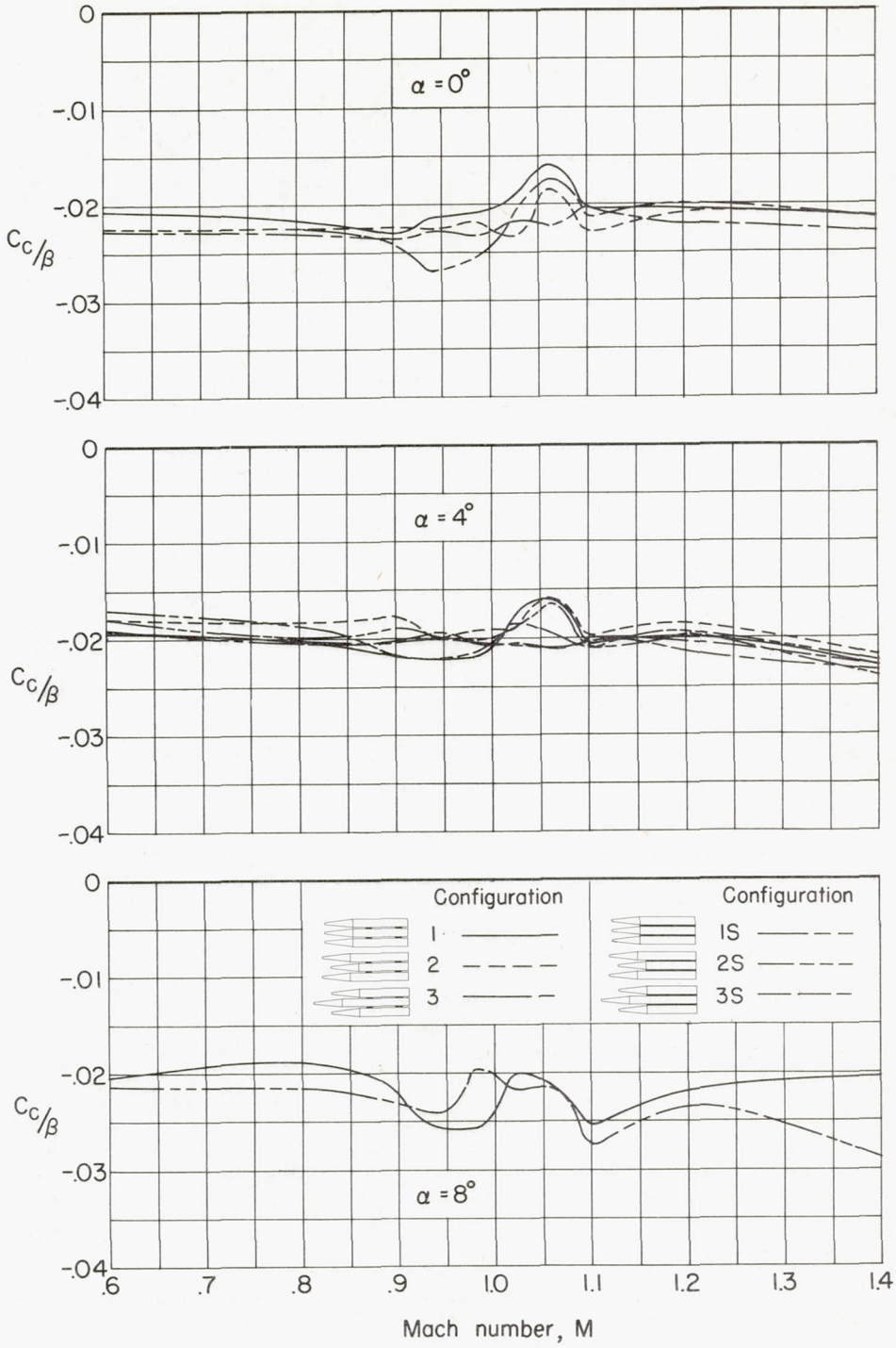

(a) $\beta = 0°$

Figure 5.- Variation of C_c/β with Mach number at constant angles of attack and sideslip for several triple-body configurations.

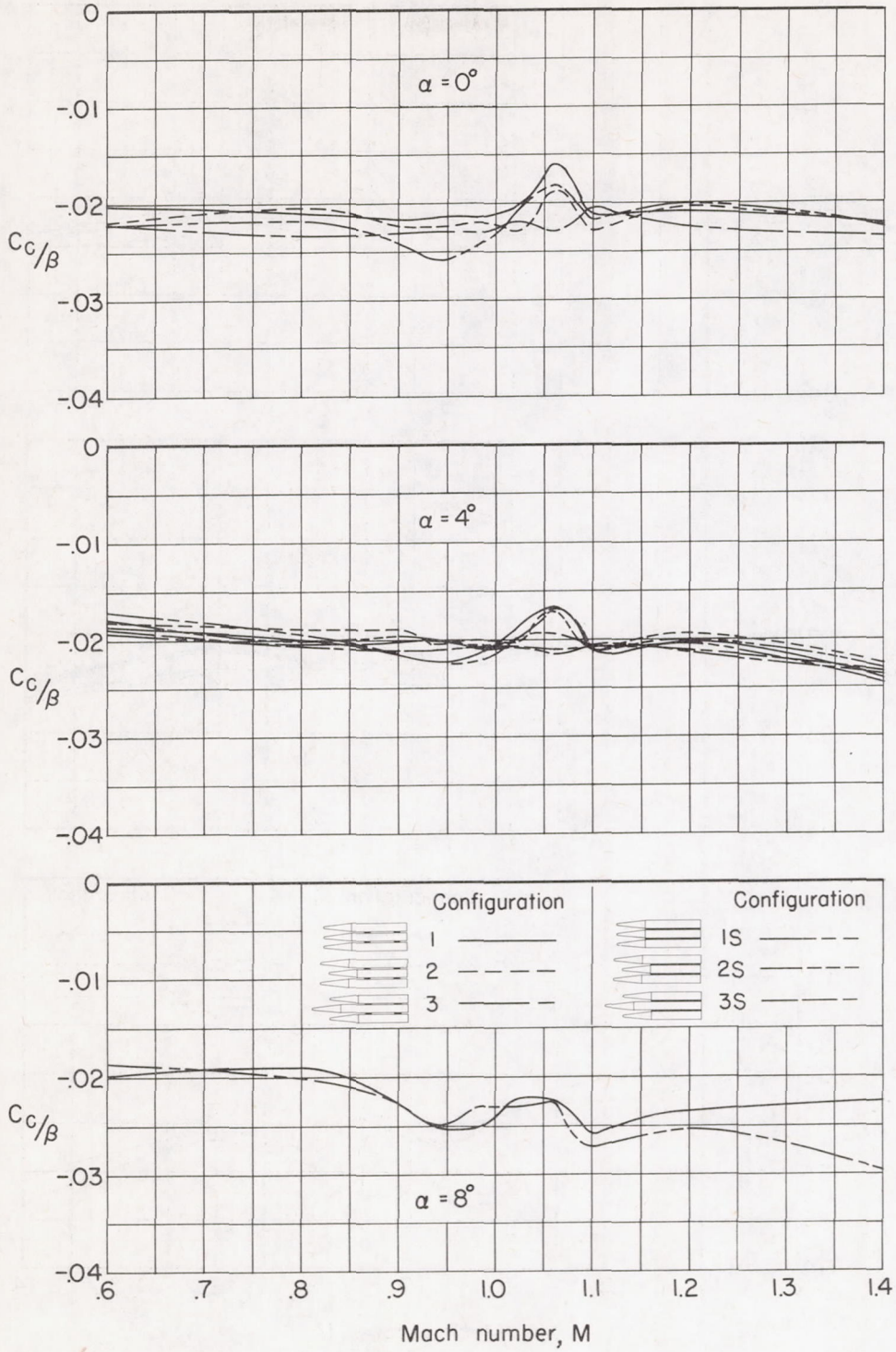

(b) $\beta = 3°$

Figure 5.- Continued.

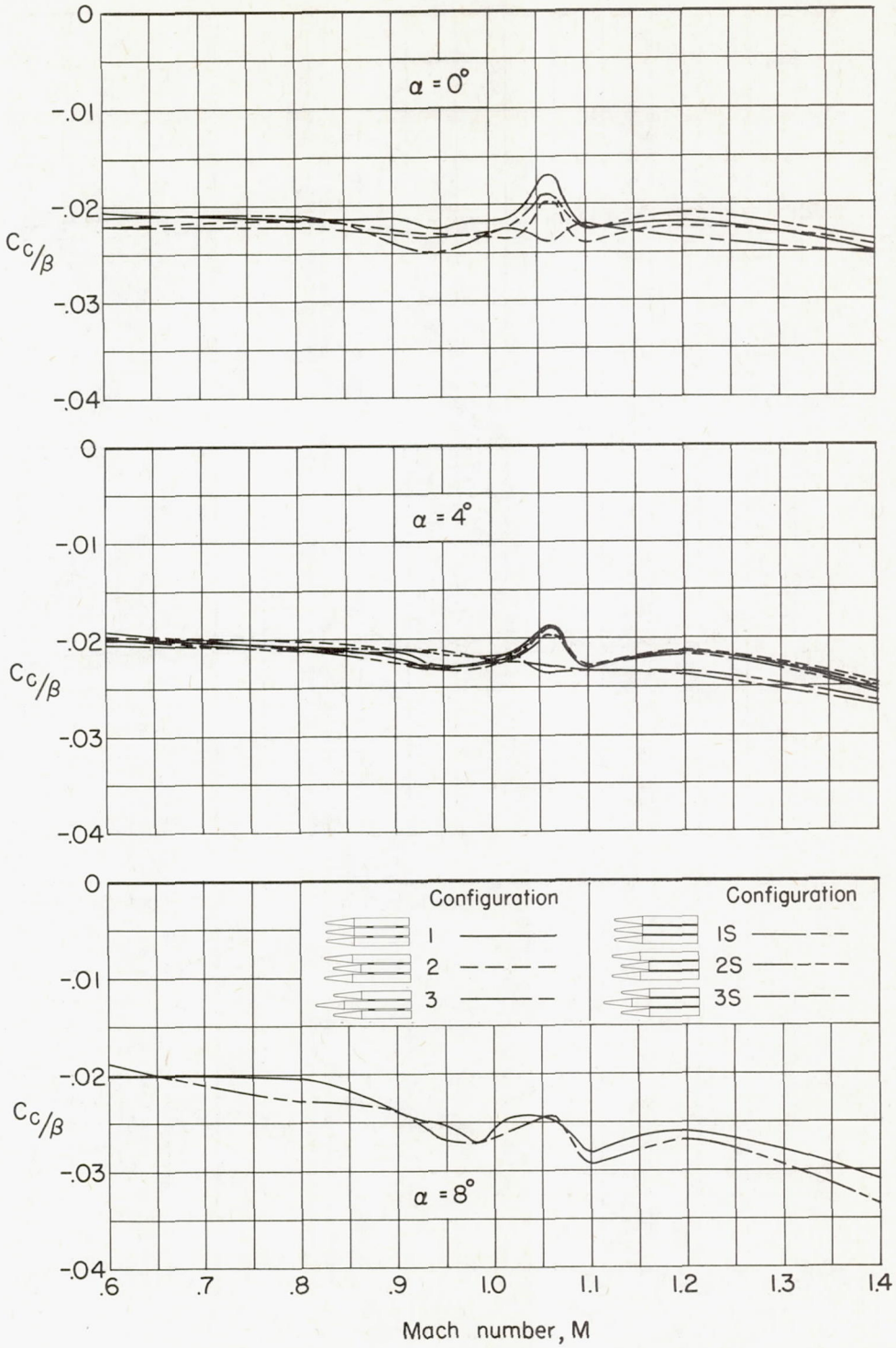

(c) $\beta = 6°$

Figure 5,- Concluded.

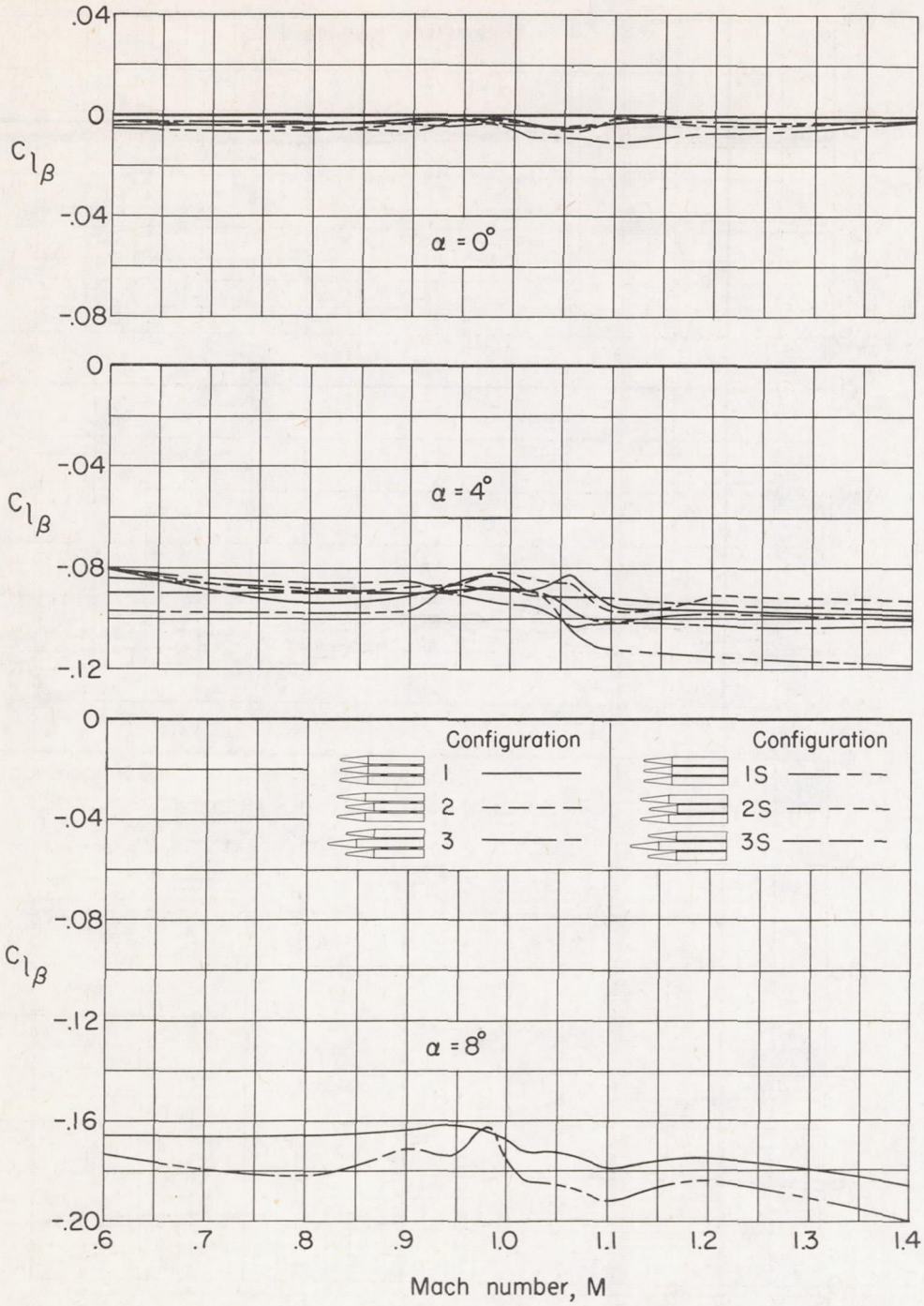

(a) $\beta = 0°$

Figure 6.- Variation of C_{l_β} with Mach number at constant angles of attack and sideslip for several triple-body configurations.

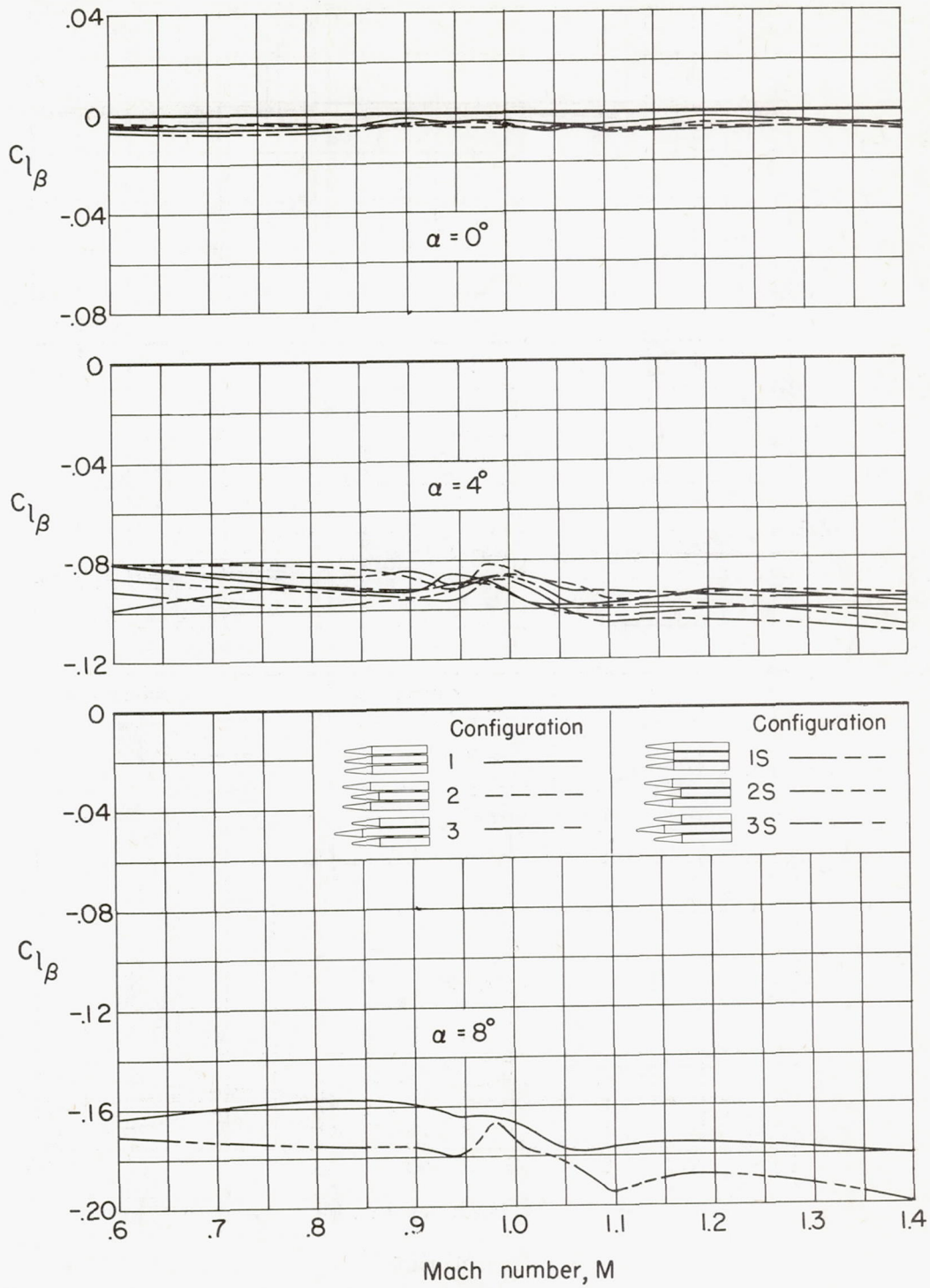

(b) $\beta = 3°$

Figure 6.- Continued.

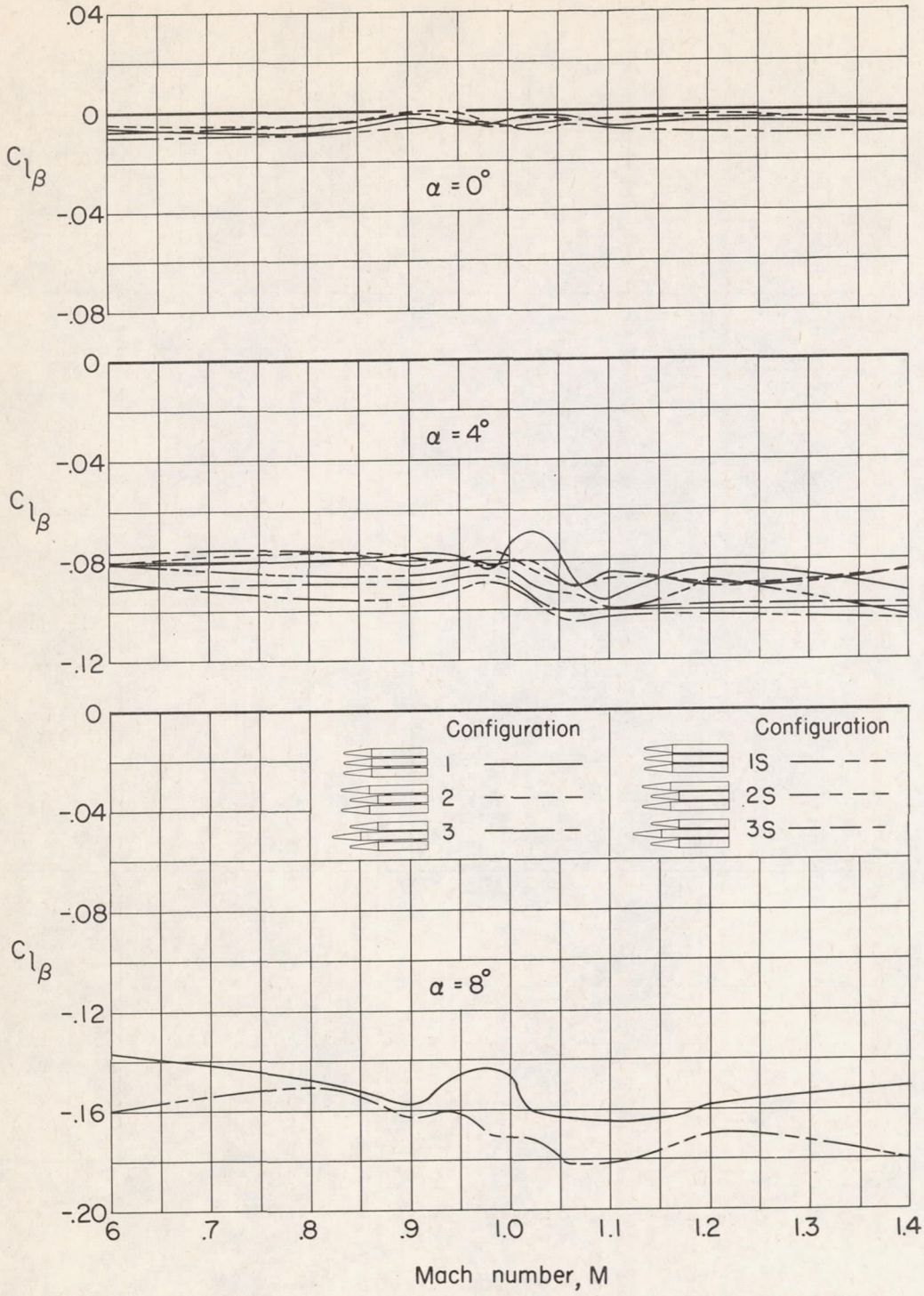

(c) $\beta = 6°$

Figure 6.- Concluded.

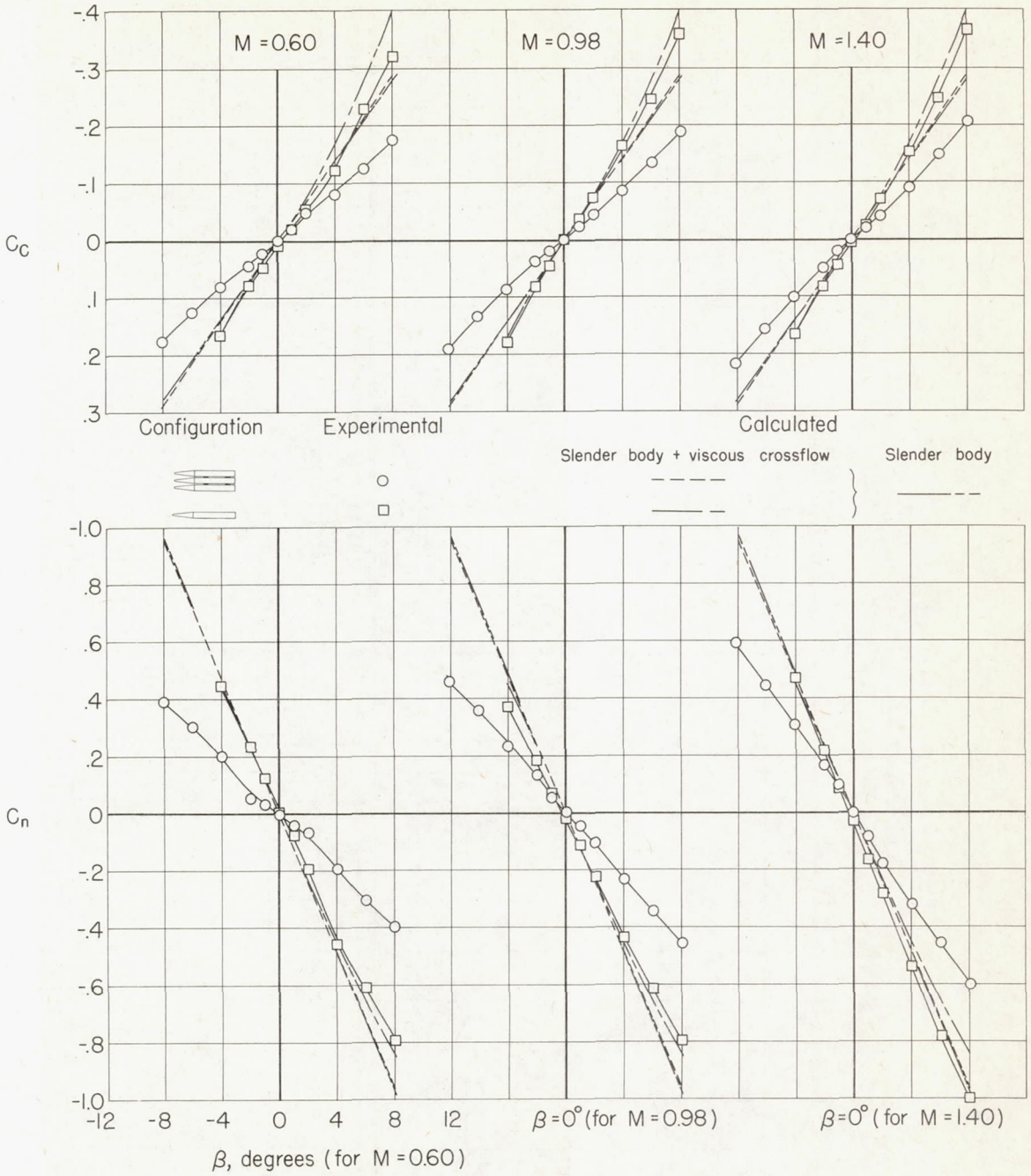

Figure 7.- Comparison of experimental cross-wind force and yawing moment with calculated values for zero lift.